

ENERGY BANDWIDTH ENHANCEMENT BY DISPERSION CORRECTION AT FLASH

E. Prat, W. Decking, T. Limberg, DESY, Hamburg, Germany

Abstract

This paper studies the impact of transverse dispersion on the SASE radiation power sensitivity with respect to the electron beam energy off-set. Both measurements and simulations are presented. By correcting the spurious dispersion inside the undulator region, the electron beam energy bandwidth is increased considerably, which decreases the SASE power jitter due to electron energy fluctuations.

INTRODUCTION

FLASH

FLASH (Free electron LASer in Hamburg), based on the TTF (TESLA Test Facility), is a user facility at DESY and a pilot facility for the European XFEL and the International Linear Collider (ILC) projects [1]. It generates SASE-FEL radiation with a wavelength ranging from the vacuum ultraviolet to the soft x-ray regime.

A schematic layout of FLASH is shown in Fig. 1. FLASH operates in pulsed mode with a macropulse repetition rate of up to 5 Hz. Each macropulse is 0.8 ms long. Within each macropulse there can be up to 800 bunches separated by 1 μ s.

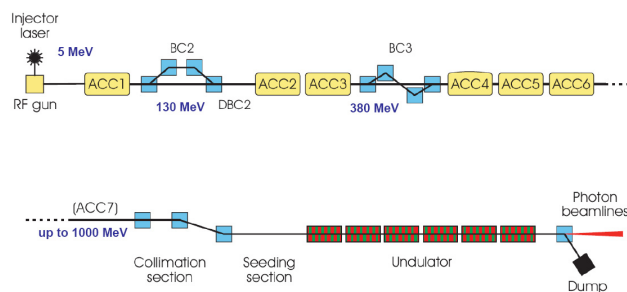


Figure 1: Schematic layout of FLASH (not to scale).

Electron bunches are generated in a laser-driven RF gun with a nominal bunch charge of 1 nC. The electron beam energy can be presently increased up to 1 GeV in six TESLA accelerating modules, each of them containing eight superconducting cavities. This maximum energy corresponds to a radiation wavelength of 6.4 nm. A further energy upgrade is planned in late 2009.

The electron bunches are longitudinally compressed in two bunch compressor chicane to reach the peak current necessary for the SASE process. The first bunch compressor (BC2) is located after the first accelerating section ($E = 127$ MeV) and can reduce the bunch length by up to about a factor of 10. The second bunch compressor (BC3) is placed after the accelerator modules

ACC23 ($E = 450$ MeV) and can further compress the beam by about a factor of 4. In total, the bunch compression system of FLASH can reduce the initial bunch length after the gun of 2 mm down to 50 μ m (RMS values), corresponding to a final design peak current of 2.5 kA.

A third-harmonic cavity which will optimize the longitudinal compression is foreseen to be installed in late 2009. After the modules that provide the final acceleration ($E = 1$ GeV) there is a collimation section that protects the undulator from radiation damage. This is done by removing electrons with large betatron amplitudes and with energy deviation larger than ± 3 %.

The undulator section consists of six permanent magnet undulators with a length of 4.5 m each. The gap is fixed at 12 mm, the peak magnetic field is 0.486 T, and the undulator period is $\lambda_u = 27.3$ mm. A pair of quadrupoles placed between each of the six modules provide the focusing required to keep the beam size in the whole section both small and constant as possible.

A dipole magnet after the undulator section deflects the electron beam into a dump, while the FEL radiation propagates to the experimental hall. In order to facilitate machine commissioning and to perform accelerator component experiments the beam can bypass the collimator and undulator sections.

Dispersion Measurement

Dispersion measurement is based on measuring the trajectory for different energies of the beam, obtained by changing the gradient of the different accelerator modules in the machine (ACC1, ACC23 and ACC456).

To compensate the kick produced by the module when its gradient is varied an orbit correction is performed just downstream the accelerator module. The horizontal and vertical-orbit readings downstream of this correction can be expressed up to second order as:

$$\begin{aligned} x(s) &= x_0(s) + D_x(s_0, s)\delta + D_{xx}(s_0, s)\delta^2 \\ y(s) &= y_0(s) + D_y(s_0, s)\delta + D_{yy}(s_0, s)\delta^2 \end{aligned}$$

where $\delta = \Delta p/p_0$ is the relative momentum (or energy) deviation induced in the accelerator module, s_0 is the position of the second BPM used for the RF steering correction after the module, and s the position of any other BPM. The horizontal and vertical trajectories (x_0 and y_0) as well as the first and second-order dispersion functions (D_x , D_y , D_{xx} , D_{yy}) are obtained by a second-order polynomial fit to the BPM data.

Figure 2 displays an example of a dispersion measurement for a single BPM.

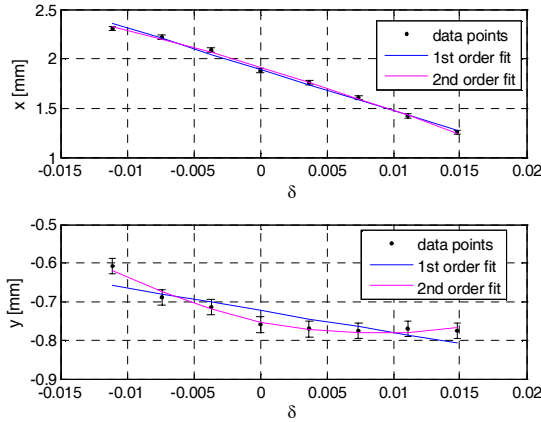


Figure 2. Example of a dispersion measurement at a single BPM at FLASH.

Uncertainties in the dispersion measurement include both statistical and systematic errors. The statistical error depends on the trajectory uncertainties, the total energy range of the measurement, and the number of steps into which the measurement is divided. For typical measurement parameters statistical uncertainties are usually in the order of 1-3 mm. Systematic errors are dominated by BPM calibration errors and are overall estimated by about 6 %.

Dispersion Correction

Both orbit and dispersion are corrected using correction coils and quadrupole movers in the undulator and collimator sections. The optimal settings are calculated using the orbit and dispersion response matrices, which are defined as the shift of the orbit or dispersion due to a change of the corrector strength:

$$OR_{i,j} = \Delta x_i / \Delta \theta_j \quad DR_{i,j} = \Delta D_i / \Delta \theta_j$$

where Δx_i and ΔD_i is the change of the orbit and dispersion in the BPM i , and $\Delta \theta_j$ is the change of the strength of the corrector j .

The algorithm consists in finding a setting of correctors $\underline{\Delta \theta}$ which induces some orbit and dispersion that minimizes in a least squares sense the difference between the final orbit and the dispersion with respect to some desired values:

$$(1-w^2) \cdot \left\| \underline{x}_{meas} + \underline{OR} \cdot \underline{\Delta \theta} - \underline{x}_{gold} \right\|^2 + w^2 \cdot \left\| \underline{D}_{meas} + \underline{DR} \cdot \underline{\Delta \theta} - \underline{D}_{gold} \right\|^2 = \min$$

where the subindex *meas* refers to the measured values and the subindex *gold* refers to the final desired orbit and dispersion. w is a factor between 0 and 1 that defines the relative weight for the orbit and the dispersion correction.

At FLASH, two quadrupole magnets (Q3/5ECOL) are used to correct the first order horizontal dispersion generated in the dipole magnets of the collimator section. Therefore, the horizontal dispersion downstream of the collimator can be modified by changing the field of Q3/5ECOL.

More details about dispersion measurement and correction at FLASH can be found in [2].

MEASUREMENTS

In order to show the reduction of the FEL power sensitivity to the electron beam energy when dispersion is corrected, the SASE macropulse energy was measured for four different dispersion scenarios as a function of the beam electron energy offset:

- Initial situation. RMS dispersion in the undulator was 22 mm in the horizontal plane and 30 mm in the vertical one.
- Extra horizontal dispersion. Additional horizontal dispersion was introduced by changing the current of the quadrupole magnets in the collimator section (Q3/5ECOL), resulting in an RMS value in the undulator of 48 mm. Vertical dispersion remained almost the same (28 mm).
- Horizontal dispersion corrected. The collimator quadrupole currents were adjusted to reduce the horizontal dispersion. Final value was 12 mm, and 31 mm in the vertical plane.
- Horizontal and vertical dispersion corrected. Starting from the previous conditions, vertical steerers from upstream of the dogleg up to the seed section were adjusted to correct vertical dispersion. Final RMS values in the undulator were 11 mm in the horizontal direction and 5 mm in the vertical one.

Figure 3 shows measured dispersion from ACC456 in the undulator BPMs for the different dispersion conditions.

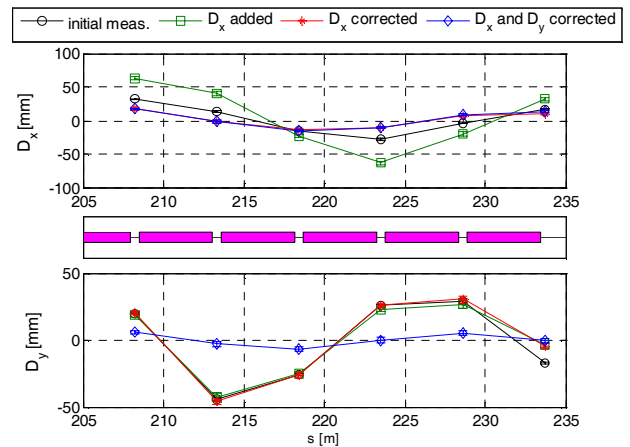


Figure 3: Measured dispersion in the undulator for the different experimental conditions.

Figure 4 shows the results of the experiment. The initial electron energy was 495 MeV and the electron charge was 0.85 nC. The plotted SASE energies are averaged over 100 shots. Although units were chosen arbitrarily to make the comparison easier, maximum SASE macropulse energy was similar in both cases: 49 μJ before dispersion correction and 40 μJ afterwards – measured by the MCP (Multi-Channel Plate) detector of FLASH [3]. The different electron energies were obtained by changing the gradient of the accelerator modules ACC456.

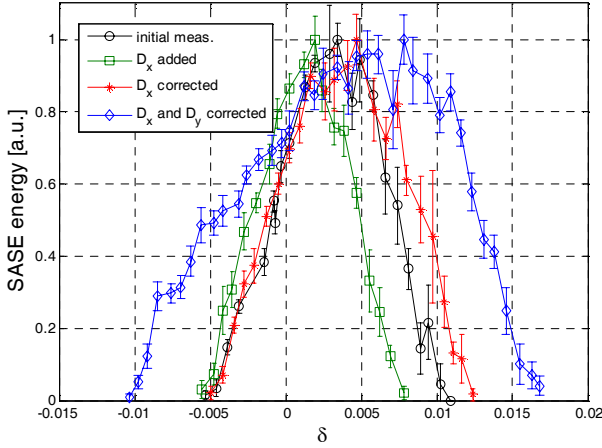


Figure 4: Measured SASE energy as a function of electron beam energy offset ($\delta = \Delta p/p_0$) for the different experimental conditions.

Initially, the FWHM (Full Width Half Maximum) of the SASE energy distribution in terms of relative electron energy deviation was 0.82 %. Adding horizontal dispersion reduced the FWHM down to 0.74 %, and correcting it increased the value up to 1.06 %. After correcting the dispersion in both planes, the final FWHM was 1.72 %. Table 1 shows a summary of the experimental results.

Table 1: Summary of the Measurements

Condition	D_x (RMS)	D_y (RMS)	FWHM in δ
Initial measurement	22 mm	30 mm	0.82 %
D_x generated	48 mm	28 mm	0.74 %
D_x corrected	12 mm	31 mm	1.06 %
D_x and D_y corrected	11 mm	5 mm	1.72 %

After dispersion correction, the SASE power sensitivity to electron beam energy offset was improved by more than a factor of two compared to the initial conditions. In other words, the range in which the radiation wavelength can be tuned by only changing the electron beam energy was increased: the wavelength could be tuned (keeping more than 50 % of the radiation power) within a range of

± 1.64 % for the initial conditions and up to ± 3.44 % after dispersion correction by simply changing the ACC456 gradient.

SIMULATIONS

Time-dependent 3-dimensional simulations of these measurements were performed with Genesis 1.3 [4]. Only the initial case and the situation after dispersion correction in both planes were considered.

The input electron beam used in the simulations for the reference point has been obtained from start-to-end simulations done for FLASH at 495 MeV and 0.85 nC using CSRtrack [5] for the bunch compressors and the collimator section and ASTRA [6] for the remainder of the lattice.

The rest of the conditions are characterized by the following differences with respect to the reference beam:

- Centroid energy change. Genesis 1.3 calculates only the FEL power in a certain bandwidth around the resonant radiation wavelength. Due to that, the resonant wavelength should be changed together with the electron energy to avoid an artificial decrease of the output radiation power. An equivalent but easier solution was adopted instead: neither the electron energy nor the resonant radiation wavelength were modified, but all the external parameters (trajectory, optics, undulator field and focusing) were scaled accordingly.
- Trajectory deviation according to energy variation and dispersion:

$$\Delta u = D_u \cdot \delta$$

$$\Delta u' = D'_u \cdot \delta$$

where u refers both to x and y . D_u and D'_u have been obtained at the entrance of the undulator from the dispersion measurements in the first two undulator BPMs. For that, the following equation for the dispersion propagation has been used for the horizontal plane (assuming that no dispersion is generated between the first two undulator BPMs):

$$D_x(s_2) = D_x(s_1)R_{11}(s_1, s_2) + D'_x(s_1)R_{12}(s_1, s_2)$$

$$D'_x(s_2) = D_x(s_1)R_{21}(s_1, s_2) + D'_x(s_1)R_{22}(s_1, s_2)$$

where $R_{ij}(s_1, s_2)$ are the elements of the linear transfer matrix R from s_1 to s_2 [7]. The vertical dispersion functions are obtained accordingly. Figure 5 shows measured and reconstructed dispersion values for both scenarios (initial case and after correction). A good agreement is observed, which also indicates that no dispersion is created inside the undulator section.

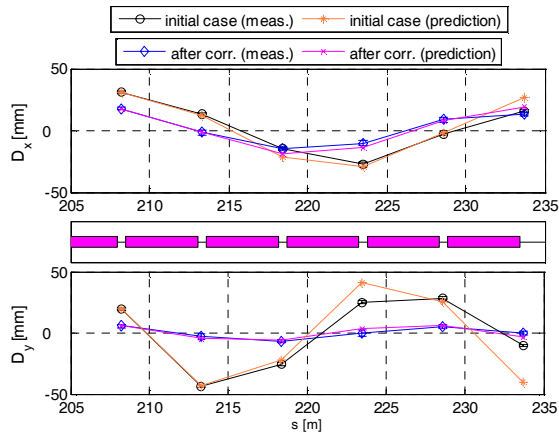


Figure 5: Measured and reconstructed dispersion along the undulator before and after dispersion correction.

- Optics variation. Since the magnet currents were not scaled, the optics at the entrance of the undulator have been re-calculated according to the energy variation.

Figure 6 shows measured and simulated SASE energy versus electron beam energy deviation. A good agreement between measurements and simulations is observed, showing the increase of the FWHM of the SASE energy distribution in terms of δ when the dispersion is corrected.

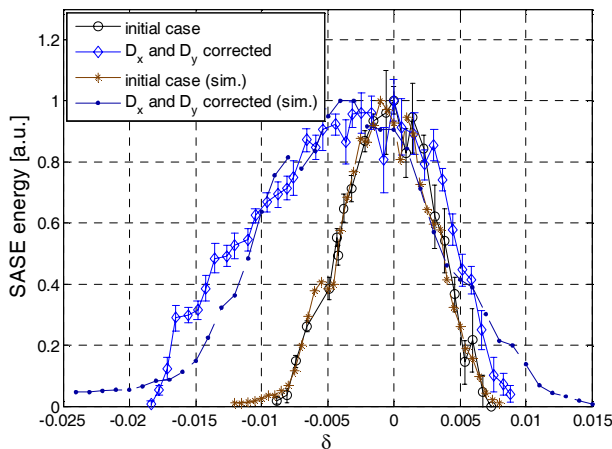


Figure 6: Measurements and simulations of SASE energy as a function of electron energy offset before and after dispersion correction.

CONCLUSION

In this paper it has been shown that dispersion correction reduces the SASE energy sensitivity to the electron beam energy offset. In other words, when dispersion is corrected there is a reduction of the undulator orbit launch sensitivity to the energy jitter. As a consequence, the beam operation is more stable, the tolerances for the RF amplitude and the phase jitter can be

more relaxed, and the radiation wavelength can be tuned in a wider range by simply changing the electron beam energy.

REFERENCES

- [1] J. Rossbach, "A VUV free electron laser at the TESLA test facility at DESY." *Nuclear Instruments and Methods in Physics Research Section A* 375, 269-273, 1996.
- [2] E. Prat, *Spurious Dispersion Effects at FLASH*, PhD thesis, University of Hamburg, 2009.
- [3] A. Bytchkov et al., "Development of MCP-based photon diagnostics at the TESLA Test Facility at DESY." *Nuclear Instruments and Methods in Physics Research Section A* 528, 254-257, 2004.
- [4] S. Reiche, *GENESIS 1.3 User Manual*, 2004.
- [5] M. Dohlus and T. Limberg, *CSRtrack Version 1.2 Users Manual*. DESY, Hamburg, Germany.
- [6] K. Floetmann, *ASTRA - A Space Charge Tracking Algorithm*. DESY, Hamburg, Germany.
- [7] K. L. Brown, *A First- and Second-Order Matrix Theory for the Design of Beam Transport Systems and Charged Particle Spectrometers*. SLAC Report-75, SLAC, Menlo Park, USA, 1982.